

Two-dimensional angular optical scattering patterns of microdroplets in the mid infrared with strong and weak absorption

Kevin B. Aptowicz, Yong-Le Pan, and Richard K. Chang

Department of Applied Physics, Yale University, New Haven, Connecticut 06520

Ronald G. Pinnick, Steven C. Hill, and Richard L. Tober

U.S. Army Research Laboratory, Adelphi, Maryland 20783

Anish Goyal and Thomas Jeys

MIT Lincoln Laboratory, Lexington, Massachusetts 02420

Burt V. Bronk

U.S. Air Force Research Laboratory at Edgewood Chemical and Biological Center, Aberdeen Proving Ground, Maryland 21010

Received April 16, 2004

Two-dimensional angular optical scattering (TAOS) patterns of droplets composed of a mixture of H₂O and D₂O are detected in the mid infrared. First, a lens is used in the Abbé sine condition to collect a small solid angle of light, where the scattering pattern matches well numerical simulations based on Mie theory. Next, TAOS patterns from droplets spanning a large ($\approx 2\pi$ sr) solid angle are captured simultaneously at two wavelengths. The effects of absorption are evident in the patterns and are discernible without the need for curve matching by Mie theory. © 2004 Optical Society of America

OCIS codes: 000.1570, 010.1100, 290.3030, 290.4020, 290.5850.

From microbiology to astrophysics, the scientific community has long embraced light scattering from small particles as a diagnostic tool. Recently the use of light scattering to probe single chemical and biological aerosols has been greatly enhanced by use of an ellipsoidal reflector in conjunction with a CCD or an intensified CCD detector to capture angularly resolved scattered light over a solid angle approaching 2π sr.^{1–3} These light-scattering patterns, and even those over smaller solid angles, provide substantial information about the scattering particle because the detected patterns depend on the particle's morphology (size, shape, and internal structure) and composition. For instance, with certain restrictions on the particle, the solution of the inverse-scattering problem of extracting a particle's shape and size from an angular intensity distribution has been successfully demonstrated.^{2–6} Efforts have been made to extract information about particle internal structure such as whether a cluster is composed of polystyrene latex spheres or of *Bacillus subtilis* spores.^{1,7} Finally, the optical composition of droplets, i.e., the complex refractive index ($m = n + ik$), was estimated by curve matching of the angular scattering data collected over a small solid angle to numerical simulations based on Mie theory.⁸

In this Letter we extend these angularly resolved elastic scattering techniques into the mid-infrared wavelength regime, where there are strong absorption bands that arise from fundamental molecular vibrational modes of common atmospheric aerosol constituents. This absorption strongly affects angular scattering and provides an additional parameter with which to characterize aerosols that is directly related

to molecular structure. Although these techniques are being developed for point detection, the data collected in the atmospheric transmission windows at 3–5 and 8–12 μm can also be applied to the modeling and understanding of results from stand-off detection systems such as lidar.

Two experiments were conducted. The first utilized a lens in the Abbé sine condition to detect the two-dimensional angular optical scattering (TAOS) pattern of single droplets. We then compared these TAOS patterns with Mie theory predictions to deduce the imaginary index from the best fit. However, Mie theory does not extend to inhomogeneous particles or to nonspherical particles or aggregates. To analyze such particles we conducted a second experiment in which TAOS patterns at two different wavelengths were simultaneously detected from a single aerosol particle. Because the two TAOS patterns were collected simultaneously on the same particle, the particle's orientation and morphology were identical for both scattering events, thereby allowing the absorption-based variations in the patterns to be prominent. Both systems detect the scattered light *in situ* and in real time.

The coordinate system used throughout this Letter is shown in Fig. 1(a) and is described in Ref. 1. A simplified schematic of the first experimental arrangement for extracting the imaginary part of the refractive index of a spherical particle is shown in Fig. 1(b). A liquid-dispenser system (MicroDrop GmbH) based on piezo technology generated droplets from an exit orifice (41- μm diameter) at a rate of ~ 500 Hz. The droplet diameter varied from 54 to 57 μm . The droplets were composed of three solutions: distilled water (H₂O),

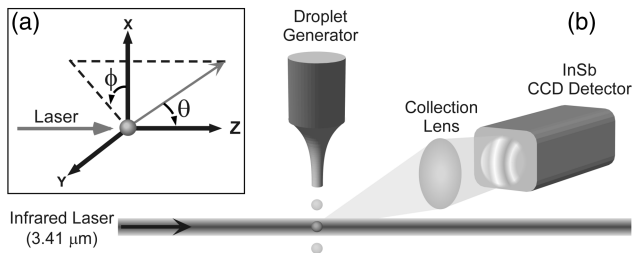


Fig. 1. (a) Spherical polar coordinates system used to define the direction of a scattered ray. (b) Experimental setup utilized for TAOS measurements.

deuterium oxide (D_2O), and a 50%–50% mixture of H_2O and D_2O .

The laser source was a type II InAs–GaInSb interband cascade laser operating in cw mode to generate light at a wavelength of 3.41 μm with optical powers approaching 40 mW.^{9,10} The emission from the facet of the semiconductor cavity was quite divergent, requiring an $f/1$ CaF_2 biconvex lens to collimate the emitted light. In addition, although this is not apparent in Fig. 1(b), an $f/3.75$ ZnSe biconvex lens focused the collimated light onto the droplet to increase signal intensity. An $f/2$ CaF_2 plano–convex lens collimated the scattered light onto the detecting focal plane array. The lens's optic axis was at $\theta = 35^\circ$ and $\phi = 270^\circ$; the laser beam was polarized along the x axis.

The angular range of collected light spanned 23° from $\theta = 23.5^\circ$ to $\theta = 46.5^\circ$. However, because of severe spherical aberrations in the outer limits of the angular range the practical collection range was 26° – 42° . These effects were mitigated by an exact ray-trace of the system calculated in Matlab. The detector, an InSb 320×256 focal-plane array (Santa Barbara Focal Plane), was run at a frame rate of 63.13 Hz with an integration window of 217 μs such that only a single scattering event would be detected.

A TAOS pattern for each type of solution is shown in Figs. 2(a)–2(c). The effects of spherical aberration can be noted by the increase in intensity near the perimeter of the TAOS pattern. There is also readout noise that manifests itself in the TAOS patterns as horizontal lines. In addition, as the laser intensity fluctuated throughout the experiment, the absolute intensity between TAOS patterns cannot be compared. A vertically binned (45 pixels) horizontal slice from each type of TAOS pattern is plotted in Figs. 2(d)–2(f), together with analytical data based on Mie theory. We estimated the droplet diameters with which to calculate the Mie theory curves by measuring an accumulated volume of droplets generated at the chosen frequency over a fixed time; complex refractive-index values were taken from the literature.¹¹ To calculate the complex refractive index of the H_2O – D_2O mixture we took a linear average of the H_2O and D_2O refractive indices. There is an inaccuracy of as much as 1° in the procedure used to measure the scattering angles; thus the angle range was slightly shifted ($<1^\circ$) from the measured values to fit the data to theory. The experimental data show a good match with numerical data based on Mie theory, although the residual effects of spherical aberration can be seen at the edges of

the plotted angular range. Because of the spherical aberrations in the TAOS patterns and the inaccuracies in the scattering angles and droplet diameters, the data were not sufficiently accurate to allow us to determine a particle's absorptivity by comparing the experimental angular scattering with theory.

The scheme for collecting TAOS images at two wavelengths simultaneously is shown in Fig. 3. The two laser sources were optically pumped GaSb-based semiconductor lasers with type II InAs–InGaSb quantum-well gain regions emitting at 3.9 and 5.1 μm with a peak power of ~ 0.4 W and a pulse duration of 100 μs .^{12,13} Both wavelengths are relatively transparent in H_2O , but D_2O has relatively high absorption at 3.9 μm while being transparent at 5.1 μm . For D_2O the imaginary component of the refractive index is 0.260 at 3.9 μm , in contrast to 0.002 at 5.1 μm . We utilized beam-shaping optics (spherical and cylindrical lenses) as well as an $f/3.75$ CaF_2 focusing lens to achieve a desired spot size of $50 \mu\text{m} \times 500 \mu\text{m}$, where the major axis is perpendicular to the propagation direction of the droplet. The polarizations of both laser beams were perpendicular to the propagation direction of the droplets. An ellipsoidal mirror collected the backward hemisphere of scattered light ($0^\circ \leq \phi \leq 360^\circ$, $90^\circ \leq \theta \leq 163^\circ$) and focused it through a spatial filter located at the ellipsoid's second focal point. To reduce aberration effects, an $f/1$ ZnSe aspheric lens collimated the scattered light, after which the two wavelengths were separated by a dichroic mirror. Finally, a biconvex $f/1$ CaF_2 lens coupled the scattered light onto the InSb detectors.

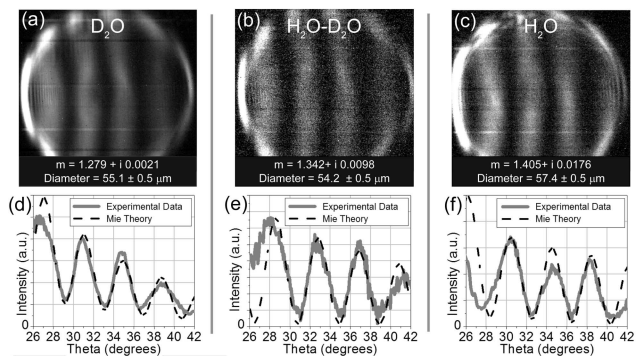


Fig. 2. Typically detected TAOS patterns from droplets composed of D_2O , a 50%–50% mixture of H_2O and D_2O , and H_2O . (d)–(f) Horizontal slices of collected TAOS patterns compared with Mie theory calculations.

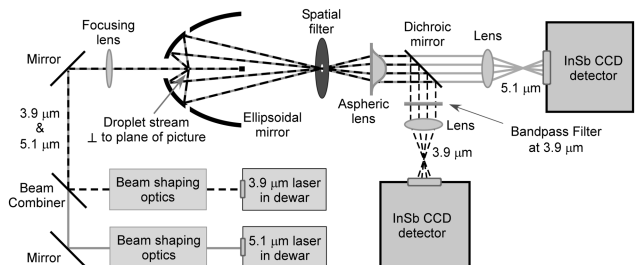


Fig. 3. Experimental setup for collecting simultaneous TAOS patterns at two wavelengths.

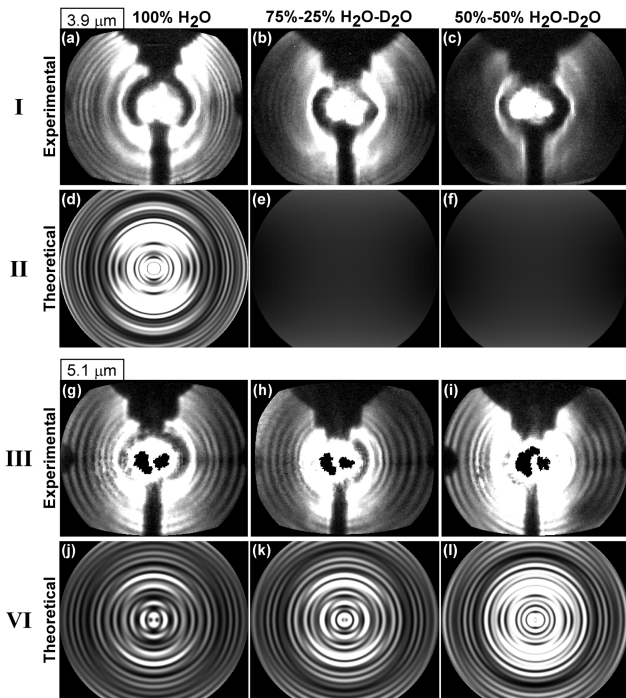


Fig. 4. Row I, TAOS pattern at $\lambda = 3.9 \mu\text{m}$ detected from a single droplet (diameter, $\sim 55 \mu\text{m}$). Row II, corresponding numerical simulations based on Mie theory. Row III, TAOS patterns collected simultaneously at $5.1 \mu\text{m}$ from the same single droplets as for row I. Row IV, corresponding numerical simulations of row III based on Mie theory.

Droplets from three different mixtures of $\text{H}_2\text{O}-\text{D}_2\text{O}$ were analyzed: 100%–0%, 75%–25%, and 50%–50%. The experimentally collected data, as well as numerical simulations based on Mie theory, are shown in Fig. 4. There are several experimental artifacts embedded in the TAOS patterns because of (1) the shadow of the droplet generator nozzle protruding into the ellipsoidal mirror; (2) the shadow of the beam block mount; and (3) the diffraction of the illuminating laser beam about the beam block. Note that we processed the patterns to be linear in θ by taking into account the optical arrangement of the system.

The TAOS patterns shown in Fig. 4 were collected from single droplets illuminated simultaneously by the two collinear 3.9- and 5.1- μm laser beams. Each column in Fig. 4 indicates a different $\text{H}_2\text{O}-\text{D}_2\text{O}$ droplet composition, as labeled. TAOS patterns (row I) collected at 3.9 μm show the effects of increasing the concentration of D_2O that leads to an increase in absorption. These patterns qualitatively match the numerical simulations based on Mie theory (row II), although there appears to be some discrepancy for the 75%–25% case [see Figs. 4(b) and 4(e)] that is believed to be due to oversimplification in estimating the absorption by taking a linear interpolation of known absorption values for neat fluids and ignoring effects of isotopes.¹⁴ TAOS patterns (row III) were collected simultaneously at 5.1 μm from the same single droplets. These patterns also agree with predictions from Mie theory in which there was a slight

increase in scattering intensity of the central region ($\theta > 135^\circ$) with increasing concentrations of D_2O . For the numerical simulations the droplet diameter was estimated to be 55 μm and the refractive index was gathered from the literature.¹¹ By comparing the data in row I with row III, one can clearly distinguish between droplets of pure H_2O and droplets that contain a considerable amount of D_2O by comparing the angular scattering patterns.

We acknowledge support by the RAAD program through the U.S. Army Research Laboratory (contract ARO DAAD19-02-0003), the Air Force Research Laboratory, the Air Force Material Command, and the U.S. Air Force under grants F33615-00-2-6059 and F19628-00-C-0002. The authors thank K. Gurton of the U.S. Army Research Laboratory for his input in designing and assembling the experiment, Ron Kaspi of the U.S. Air Force Research Laboratory for use of its 5.1- μm mid-infrared laser, as well as M. L. Myrick of the University of South Carolina for suggesting the use of D_2O in our studies. The views, conclusions, and recommendations reached herein are those of the authors and should not be interpreted as necessarily those of any of the government agencies sponsoring the work or employing any of the authors. K. B. Aptowicz's e-mail address is aptowicz@yale.edu.

References

1. Y. L. Pan, K. B. Aptowicz, R. K. Chang, M. Hart, and J. D. Eversole, *Opt. Lett.* **28**, 589 (2003).
2. P. Kaye, E. Hirst, and Z. Wang-Thomas, *Appl. Opt.* **36**, 6149 (1997).
3. E. Hirst, P. H. Kaye, and J. R. Guppy, *Appl. Opt.* **33**, 7180 (1994).
4. P. H. Kaye, *Meas. Sci. Technol.* **9**, 141 (1998).
5. B. Sachweh, H. Barthel, R. Polke, H. Umhauer, and H. Buttner, *J. Aerosol Sci.* **30**, 1257 (1999).
6. T. R. Marshall, C. S. Parmenter, and M. Seaver, *Science* **190**, 375 (1975).
7. S. Holler, Y. L. Pan, R. K. Chang, J. R. Bottiger, S. C. Hill, and D. B. Hillis, *Opt. Lett.* **23**, 1489 (1998).
8. M. D. Barnes, C. Y. Kung, N. Lermer, K. Fukui, B. G. Sumpter, D. W. Noid, and J. U. Otaigbe, *Opt. Lett.* **24**, 121 (1999).
9. R. Q. Yang, J. L. Bradshaw, J. D. Bruno, J. T. Pham, D. E. Wortman, and R. L. Tober, *Appl. Phys. Lett.* **81**, 397 (2002).
10. S. Suchalkin, J. Bruno, R. Tober, D. Westerfeld, M. Kisin, and G. Belenky, *Appl. Phys. Lett.* **83**, 1500 (2003).
11. J. E. Bertie, M. K. Ahmed, and H. H. Eysel, *J. Phys. Chem.* **93**, 2210 (1989).
12. A. K. Goyal, G. W. Turner, M. J. Manfra, P. J. Foti, P. O'Brien, and A. Sanchez, in *Proceedings of the IEEE Conference on Lasers and Electro-Optics Society (LEOS) Annual Meeting* (Institute of Electrical and Electronics Engineers, Piscataway, N.J., 2001), pp. 200–201.
13. R. Kaspi, A. Ongstad, G. C. Dente, J. Chavez, M. L. Tilton, and D. Gianardi, *Appl. Phys. Lett.* **81**, 406 (2002).
14. J. J. Max and C. Chapados, *J. Chem. Phys.* **116**, 4626 (2002).